Lysosomal exocytosis and caspase-8-mediated apoptosis in UVA-irradiated keratinocytes

Hanna Appelqvist, Petra Wäster, Ida Eriksson, Inger Rosdahl and Karin Öllinger

Original Publication:

Hanna Appelqvist, Petra Wäster, Ida Eriksson, Inger Rosdahl and Karin Öllinger, Lysosomal exocytosis and caspase-8-mediated apoptosis in UVA-irradiated keratinocytes, 2013, Journal of Cell Science, (126), 24, 5578-5584.
http://dx.doi.org/10.1242/jcs.130633

Lysosomal exocytosis and caspase-8-mediated apoptosis in UVA-irradiated keratinocytes

Hanna Appelqvist[1,*], Petra Wäster[1,2,*], Ida Eriksson[1], Inger Rosdahl[2] and Karin Öllinger[1,3,‡]

[1]Experimental Pathology, Department of Clinical and Experimental Medicine, Faculty of Health Sciences, Linköping University, Linköping, Sweden
[2]Dermatology and Venereology, Department of Clinical and Experimental Medicine, Faculty of Health Sciences, Linköping University, Linköping, Sweden
[3]Department of Clinical Pathology and Clinical Genetics, County Council of Östergötland, Linköping, Sweden

*These authors contributed equally to this work
‡Author for correspondence (karin.ollinger@liu.se)

Accepted 12 September 2013
Journal of Cell Science 126, 5578–5584

doi: 10.1242/jcs.130633

Summary

Ultraviolet (UV) irradiation is a major environmental carcinogen involved in the development of skin cancer. To elucidate the initial signaling during UV-induced damage in human keratinocytes, we investigated lysosomal exocytosis and apoptosis induction. UVA, but not UVB, induced plasma membrane damage, which was repaired by Ca^{2+}-dependent lysosomal exocytosis. The lysosomal exocytosis resulted in extracellular release of cathepsin D and acid sphingomyelinase (aSMase). Two hours after UVA irradiation, we detected activation of caspase-8, which was reduced by addition of anti-aSMAse. Furthermore, caspase-8 activation and apoptosis was reduced by prevention of endocytosis and by the use of cathepsin inhibitors. We conclude that lysosomal exocytosis is part of the keratinocyte response to UVA and is followed by cathepsin-dependent activation of caspase-8. The findings have implications for the understanding of UV-induced skin damage and emphasize that UVA and UVB initiate apoptosis through different signaling pathways in keratinocytes.

Key words: Keratinocyte, UV irradiation, Lysosome, Cathepsin, Endocytosis, Apoptosis

Introduction

Well-established epidemiological evidence indicates that ultraviolet (UV) irradiation is a major environmental skin carcinogen (Armstrong and Kricker, 2001), but the underlying mechanisms have still not been elucidated. In particular, the effects of the different wavelengths within the UV spectrum need to be further clarified. UVB irradiation (280–320 nm) directly induces alterations in DNA, whereas UVA (320–400 nm) alters the redox balance of the cell and induces oxidative stress and indirect DNA damage (Marrot and Meunier, 2008; Tyrrell, 1995).

The two main apoptosis signaling routes are the intrinsic pathway, characterized by the release of apoptogenic factors from the mitochondria, and the extrinsic pathway, dependent on signaling via the death receptors. These pathways generally converge in activation of the caspase family. UV-induced apoptosis is a complex process mediated by the intrinsic pathway in both melanocytes and keratinocytes (Assefa et al., 2005; Bivik et al., 2006). However, UV irradiation has also been shown to induce apoptosis by ligand-independent clustering and activation of the death receptors of the tumor necrosis factor (TNF) family (Rehemtulla et al., 1997). Alternatively, endogenous TNF-α production has been suggested to contribute to the activation of the extrinsic apoptosis pathway following UVB irradiation (Köck et al., 1990). Extrinsic apoptosis signaling is characterized by the activation of caspase-8, which directly triggers effector caspases or engages the intrinsic pathway. Death receptor signaling, including activation of caspase-8, was initially suggested to occur at the cytosolic leaflet of the plasma membrane. However, it is now clear that the death receptors require endocytosis to activate apoptotic signaling (Akazawa et al., 2009; Lee et al., 2006; Schneider-Brachert et al., 2004), and caspase-8 activation is suggested to occur at intracellular vesicles sometimes referred to as receptosomes (Tchikov et al., 2011). Nowadays, it is well known that lysosomal proteases, the cathepsins, participate in apoptosis signaling initiated both by intrinsic (Johansson et al., 2003; Roberg et al., 1999) and extrinsic pathways (Guicciardi et al., 2000).

In addition to the degradative and cell-death-inducing functions of lysosomes, these organelles have a number of other essential functions such as plasma membrane repair. This membrane restoration is a Ca^{2+}-dependent process involving rapid translocation and fusion of lysosomes resulting in the formation of a lysosomal patch (Reddy et al., 2001). Finally, the lysosomes fuse with the plasma membrane and repair the injury (McNeil, 2002). To promote resealing, the formed lesions are removed by endocytosis (Idone et al., 2008), which is triggered by extracellular release of the lysosomal enzyme acid sphingomyelinase (aSMase). aSMase generates ceramide, which clusters together into lipid rafts, enabling successful vesicular transport and signal transduction during the cellular stress response (Corre et al., 2010; Li et al., 2012; Simons and Toomre, 2000; Tam et al., 2010).

In previous studies, we have established that there is a significant contribution of lysosomes in cell death signaling, including UV-induced apoptosis (Appelqvist et al., 2012a; Bivik et al., 2006; Wäster and Öllinger, 2009). In order to further elucidate the mechanistic contribution of lysosomes in UV-induced damage, we studied the impact of lysosomal exocytosis

Journal of Cell Science

and participation of lysosomal constituents in the initial cell death signaling.

Results

Lysosomal exocytosis and caspase-8 activation after UVA irradiation

Human keratinocytes were exposed to UVA or UVB irradiation in phosphate-buffered saline (PBS) with or without Ca^{2+}. In the Ca^{2+}-free buffer, UVA exposure resulted in immediate plasma membrane damage, measured by an uptake of the membrane impermeable dye propidium iodide (PI; Fig. 1A). However, in the presence of Ca^{2+} the damage was rapidly resealed and no PI-positive cells were detected. We found that a portion of the lysosomes redistributed to the periphery of the cell (Fig. 1B) and the luminal part of lysosome-associated membrane protein-1 (LAMP-1) was detected in the vicinity of the plasma membrane in the unfixed cells directly after UVA irradiation (Fig. 1C). The appearance of LAMP-1 in the plasma membrane is a marker of the lysosomal exocytosis process (Jans et al., 2004; Reddy et al., 2001; Rodríguez et al., 1997). The translocation of LAMP-1 was accompanied by the extracellular release of the lysosomal contents, including cathepsin D (Fig. 1D) and aSMase (supplementary material Fig. S1B). The exocytosis of lysosomes has previously been found to be followed by the extracellular release of aSMase and the formation of ceramide-enriched lipid rafts (Tam et al., 2010). Directly after UVA irradiation, lipid rafts appeared in the plasma membrane (Fig. 1E). Taken together, these results support the conclusion that UVA-induced damage to the plasma membrane is repaired by lysosomal exocytosis. Directly after UVB exposure, there was no significant damage to the plasma membrane, no lipid peroxidation and no signs of lysosomal exocytosis (Fig. 1A–E; supplementary material Fig. S1A,B). The doses of UVA and UVB were chosen to induce 40–60% apoptosis after 6 hours, as detected by nuclear fragmentation (Fig. 1F, black bars). At this time point, the caspase-3 activity increased 9.5- and 4.8-fold after exposure to UVA and UVB, respectively (supplementary material Fig. S1C). Interestingly, we found that the upstream

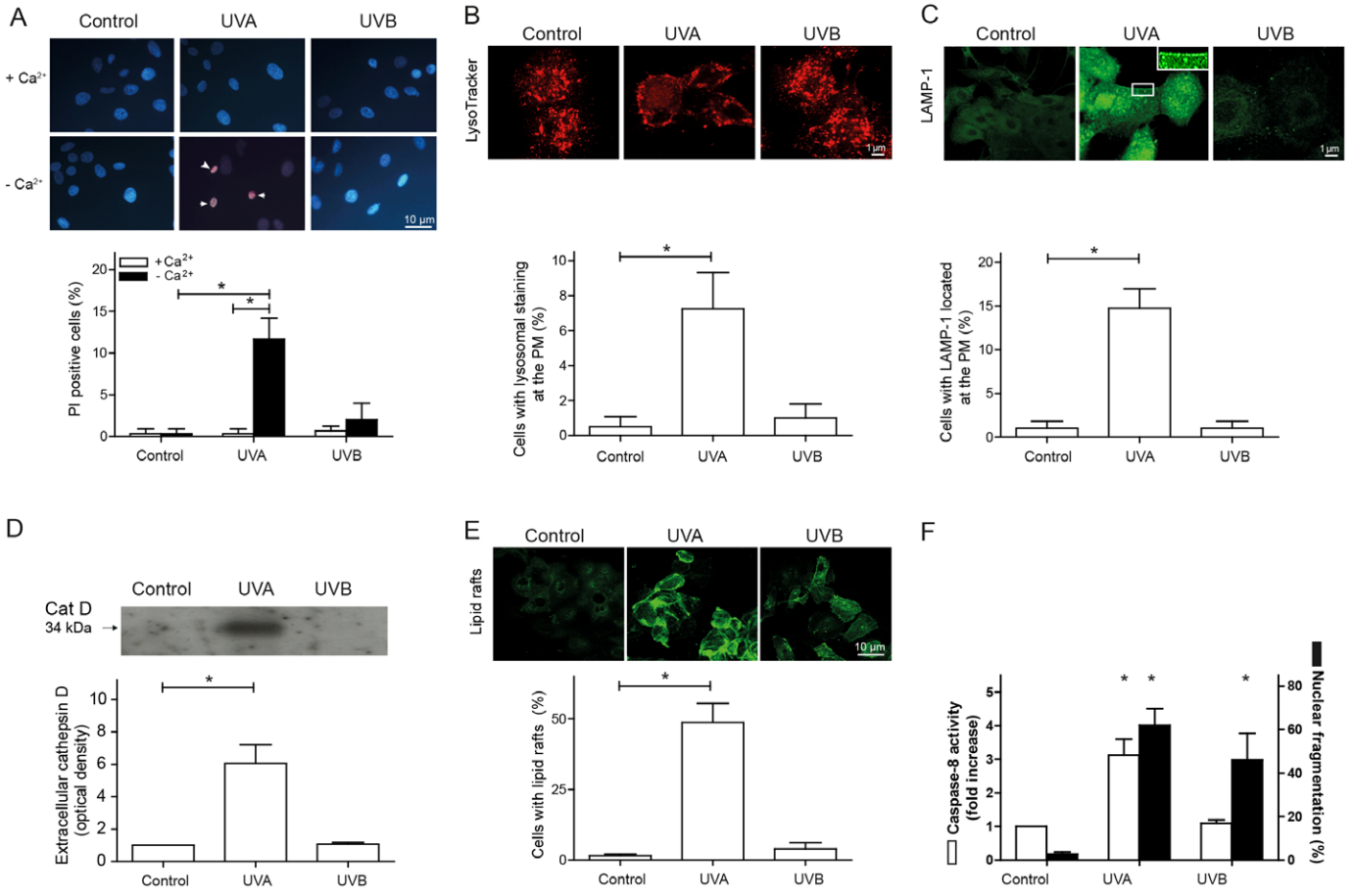

Fig. 1. UVA irradiation causes plasma membrane damage, which is repaired by lysosomal exocytosis. Human keratinocytes were exposed to UVA (60 J/cm^2) and UVB (500 mJ/cm^2) irradiation. (A) Merged images of DAPI (blue; all nuclei) and propidium iodide (PI, pink and marked with arrowheads) staining, and quantification of PI-positive cells, directly following irradiation. Irradiation was performed in the presence or absence of Ca^{2+}. PI was added to mark cells that failed to reseal their plasma membrane. (B,C) Images and quantification of (B) Lysotracker-stained lysosomes located at the plasma membrane (PM) directly after irradiation, and (C) immunolabeling of the luminal part of LAMP-1 in unfixed cells directly after irradiation. (D) Western blot analysis and optical density of the 34 kDa active form of cathepsin D released extracellularly directly after UV irradiation. (E) Images and quantification of lipid rafts, detected by cholera toxin subunit B conjugated to Alexa Fluor 488 directly after UV irradiation. *$P \leq 0.05$. (F) Caspase-8 activity measured 2 hours post-irradiation (white bars) and nuclear fragmentation quantified 6 hours after irradiation (black bars). Images in A, B, C and E were selected to display the characteristic appearance of the quantified fluorescent structure. *$P \leq 0.05$ compared to the control ($n=4$). Scale bars: 10 µm (A,E), 1 µm (B,C).

apoptosis signaling differed between UVA and UVB. Specifically, active caspase-8 was found 2 hours after exposure to UVA, but was not observed after UVB irradiation (Fig. 1F, white bars). Thus, lysosomal exocytosis and caspase-8 activation only occurred after UVA irradiation.

Impact of oxidative events and lysosomal exocytosis on caspase-8 activation

UVA-induced apoptosis was partly dependent upon caspase-8 given that pre-incubation of the cells with the caspase-8 inhibitor z-IETD-fmk resulted in reduced cell death as detected by nuclear fragmentation (Fig. 2A) and caspase-3 activity (supplementary material Fig. S1C). Addition of the caspase-10 inhibitor z-AEVD-fmk did not affect caspase-8 activity nor decrease nuclear fragmentation after UVA irradiation, indicating that the contribution of caspase-10 was negligible (supplementary material Fig. S2).

There was no statistically significant increase of endogenous TNF-α production in concentrated cell culture medium immediately following UVA irradiation or up to 6 hours later (supplementary material Fig. S3). However, caspase-8 activation might occur due to death receptor aggregation caused by photochemical reactions within the plasma membrane. Lipid peroxidation products were detected after UVA but not UVB irradiation (supplementary material Fig. S1A). Consequently, by pre-incubating the cultures with the membrane protective antioxidant α-tocopherol, UVA-induced caspase-8 activity and nuclear fragmentation were inhibited (Fig. 2B).

To further elucidate whether caspase-8 activation was downstream of the exocytosis process, we inhibited exocytosis by addition of vacuolin-1 (Liu et al., 2012) and anti-synaptotagmin VII antibodies (Reddy et al., 2001). The inhibitors significantly reduced LAMP-1 translocation to the plasma membrane (Fig. 2C; gray bars) and decreased caspase-8 activation (Fig. 2C; white bars). Prevention of lysosomal acidification by treatment with NH_4Cl also reduced exocytosis and caspase-8 activation (Fig. 2C).

Activation of caspase-8 is dependent on lysosomal cathepsins and endocytosis

After exocytosis, the plasma membrane lesion is removed by endocytosis (Idone et al., 2008). The activity of aSMase is of importance in the resealing process following lysosomal exocytosis, and aSMase activity was increased in keratinocytes after UVA irradiation (Fig. 3A). It was not affected by pre-treatment with a caspase-8 inhibitor, but increasing the lysosomal pH by exposing the cells to NH_4Cl reduced aSMase activity. To study the effect of extracellular aSMase, an anti-aSMase antibody was added during UVA irradiation, which decreased caspase-8 activity and nuclear fragmentation (Fig. 3B). Inhibition of endocytosis using monodansyl cadaverine (MDC) (Schütze et al., 1999) reduced caspase-8 activation and apoptosis significantly (Fig. 3C,D). MDC was verified to decrease endocytosis of FITC-conjugated dextran (data not shown). Similar results were obtained when using the endocytosis inhibitor phenylarsine oxide (PAO; supplementary material Fig. S4).

Using confocal microscopy, we found a time-dependent increase in active caspase-8 that colocalized with cathepsin-D- and LAMP-1-positive structures (Fig. 4A–C). Using triple immunostaining, we found that active caspase-8 mainly

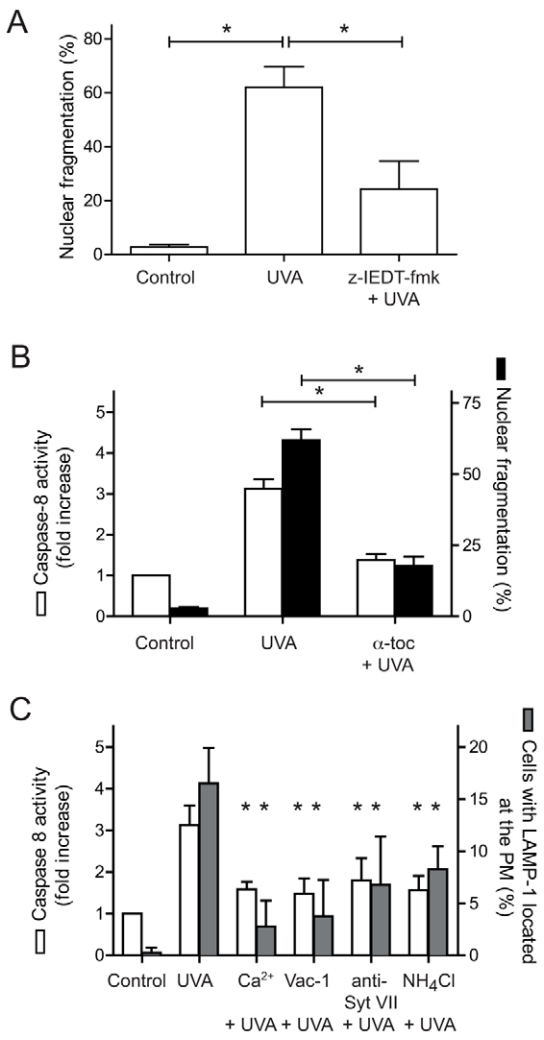

Fig. 2. Caspase-8-dependent apoptosis and increased lysosomal exocytosis in UVA-irradiated cells. Human keratinocytes were exposed to UVA irradiation (60 J/cm^2). (A) Nuclear fragmentation after 6 hours with or without pretreatment with the caspase-8 inhibitor z-IETD-fmk (40 μM, 2 hours). *$P \leq 0.05$ ($n=4$). (B) Caspase-8 activation (2 hours; white bars) and nuclear fragmentation (6 hours; black bars) after UVA irradiation, with or without pretreatment with α-tocopherol (α-toc; 10 μM, 48 hours). (C) Caspase-8 activity (2 hours; white bars) and LAMP-1 localization at the plasma membrane (PM; gray bars) analyzed directly after UVA irradiation with addition of lysosomal exocytosis inhibitors vacuolin-1 (Vac-1, 1 μM, 1 hour) and anti-Synaptotagmin VII (anti-Syt VII, 10 μg/ml) or inhibitor of lysosomal acidity (NH_4Cl; 10 mM, 30 minutes) when indicated. *$P \leq 0.05$ compared to UVA exposure ($n=4$).

appeared in the cell periphery and in vacuolar structures positive for both cathepsin D and LAMP-1 (Fig. 4D). To further analyze the endocytosis process following UVA irradiation, we added anti-aSMase antibodies or inhibited endocytosis using MDC. The colocalization of caspase-8 with LAMP-1 and cathepsin D both decreased (Fig. 4E). Furthermore, caspase-8 activity was reduced by the addition of either the cysteine cathepsin (e.g. cathepsin B and L) inhibitor E64d or the cathepsin D inhibitor pepstatin A, confirming the lysosomal involvement in caspase-8 activation (Fig. 5, white bars). Moreover, the addition of cathepsin D antibodies during

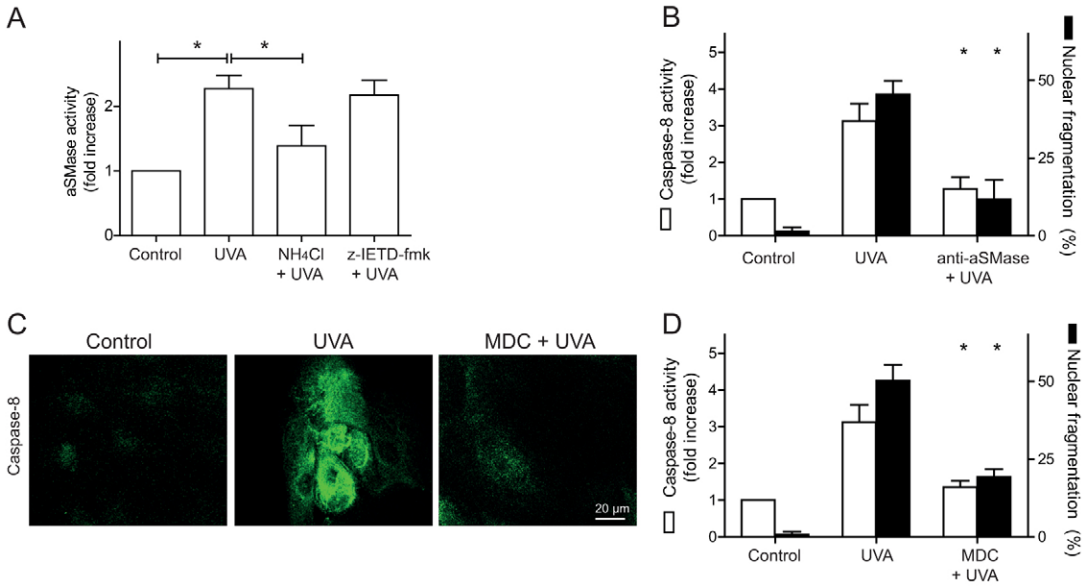

Fig. 3. Endocytosis is upstream of caspase-8 activation. Human keratinocytes were exposed to UVA irradiation (60 J/cm^2). (A) Activity of aSMase directly after UVA irradiation. When indicated, cultures were pretreated with inhibitors of lysosomal acidity (NH_4Cl; 10 mM, 30 minutes) and caspase-8 (z-IETD; 40 μM, 2 hours). *$P \leq 0.05$ ($n=4$). (B) Caspase-8 activity (2 hours; white bars) and nuclear fragmentation (6 hours; black bars) analyzed after UVA irradiation. When indicated an anti-aSMase antibody (anti-aSMase; 120 ng/ml) was added. (C) Images of active caspase-8 with or without pretreatment with the endocytosis inhibitor MDC (200 μM, 30 minutes). Images were selected to display the characteristic appearance of the quantified fluorescent structure. (D) Caspase-8 activity (white bars) and nuclear fragmentation (black bars) at 2 hours and 6 hours, respectively, after UVA irradiation with or without pretreatment with MDC. *$P \leq 0.05$ compared to UVA exposure ($n=4$).

irradiation resulted in a significant decrease in caspase-8 activation and apoptosis frequency (Fig. 5, white and black bars), indicating that caspase-8 activation is downstream of cathepsin D.

Discussion

This study presents evidence that UVA-induced plasma membrane damage in keratinocytes is rapidly repaired by Ca^{2+}-dependent lysosomal exocytosis. In contrast to the UVA findings, the plasma membrane integrity is unaffected and we found no sign of lipid peroxidation or lysosomal exocytosis after UVB irradiation. It cannot be excluded that the differences between the UVA and UVB response might be an effect of the UV doses used. This is, however, not likely because a similar level of apoptosis is detected after both UVA and UVB irradiation suggesting that the doses were properly titrated. In the present study of human keratinocytes, the early activation of caspase-8 was only detected after UVA irradiation. In contrast, in the keratinocyte-like HaCaT cell line, it has been shown that caspase-8 activation contributes to UVB-induced apoptosis (Assefa et al., 2003). In melanocytes, no initial activation of caspase-8 occurs during UVA- and UVB-induced apoptosis (Bivik et al., 2006; Wäster and Öllinger, 2009). This suggests that UV-induced caspase-8 activation is dependent on the cell type. The mechanism of irradiation-induced caspase-8 activation is still under debate. Clustering of death receptors owing to photooxidative processes in the plasma membrane or endogenous production of death receptor ligands, such as TNF-α, has been suggested (Köck et al., 1990; Rehemtulla et al., 1997). In our experimental setting, no increase in TNF-α in the cell culture medium is detected prior to caspase-8 activation. However, the protection against cell death and caspase-8 activation found after α-tocopherol pretreatment demonstrates that membrane oxidation is an important event in the signaling process. The detection of lipid peroxidation products after UVA, but not UVB, irradiation supports this view. Membrane oxidation could contribute to caspase-8 activation either by the clustering of death receptors or through other oxidative events (Assefa et al., 2005). Furthermore, the plasma membrane composition is altered by exocytosed lysosomal membranes and by ceramide production mediated by activated aSMase.

Treatment with NH_4Cl, in order to increase the pH of the lysosomal compartment, resulted in reduced caspase-8 activation. This could be an effect of reduced proteolytic activity of cathepsins but might also be an effect of decreased vesicle fusion. When adding the exocytosis inhibitors vacuolin-1 (Liu et al., 2012) and synaptotagmin-VII (Reddy et al., 2001), UVA-induced activation of caspase-8 was significantly reduced, indicating that caspase-8 activation is a downstream event in the signaling cascade. After UVA irradiation, increased activity and translocation of aSMase, as well as the formation of lipid rafts, is detected. Previously, aSMase has been found to translocate to the plasma membrane after various forms of cellular stress, such as exposure to ionizing radiation, ionophores and pore-forming bacterial toxins (Corre et al., 2010; Jans et al., 2004; Tam et al., 2010). The action of aSMase results in sphingomyelin hydrolysis and ceramide generation, which forms signaling platforms called lipid rafts (Corre et al., 2010). By adding anti-aSMase antibodies to our system, we found that inhibition of released aSMase prevented caspase-8 activation and nuclear fragmentation. In addition, by using a caspase-8 inhibitor, we demonstrate that the activity of aSMase is independent of caspase-8 activity. These findings suggest that the aSMase-dependent signaling is upstream the activation of caspase-8.

Idone et al. (Idone et al., 2008) found that exocytosis-induced alterations of the plasma membrane were followed by endocytosis to

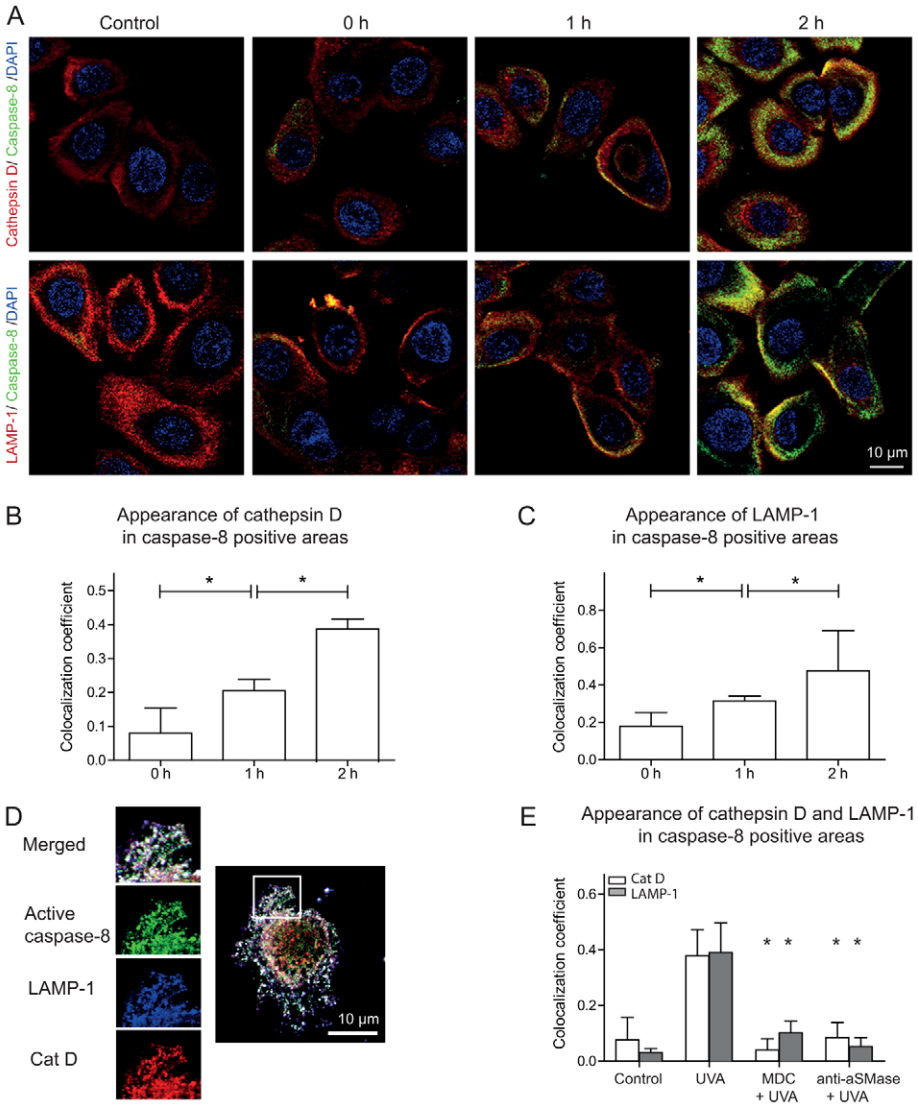

Fig. 4. Active caspase-8 colocalizes with cathepsin D and LAMP-1. (A) Merged images of immunostaining of cathepsin D or LAMP-1 (Alexa Fluor 594, red in respective images), active caspase-8 (Alexa Fluor 488, green) and nuclei stained with DAPI (blue), 1 and 2 hours after UVA irradiation (60 J/cm^2). Colocalization coefficients between (B) active caspase-8 and cathepsin D and (C) active caspase-8 and LAMP-1 (>50 cells were analyzed in each sample, n=4). *P≤0.05. (D) Immunofluorescence of a keratinocyte 2 hours after UVA irradiation and detailed images of active caspase-8 (green; Alexa 488), LAMP-1 (blue; Alexa 633) and cathepsin D (red; Alexa 594). Colocalization of all proteins in the merged image appears white. (E) Colocalization coefficients between active caspase-8, cathepsin D (white bars) and LAMP-1 (gray bars) following inhibition of endocytosis using monodansyl cadaverine (MDC; 200 µM, 30 minutes) and an aSMase antibody (anti-aSMase; 120 ng/ml) 2 hours post-irradiation (n=4). Images were selected to display the characteristic appearance of the quantified fluorescent structure. *P≤0.05 compared to UVA exposure.

restore the membrane. One hour after UVA irradiation, we found active caspase-8 in LAMP-1- and cathepsin-D-positive structures. Reducing extracellular aSMAse by anti-aSMase, and inhibition of endocytosis using MDC, prevented caspase-8 activation and consequently colocalization after UVA irradiation. Three different approaches were used to inhibit the endocytic process (treatment with MDC or PAO and addition of anti-aSMase) and all showed consistent results. We cannot, however, exclude that the acidification of endo-lysosomal system was altered and interfered with the activation of caspase-8. In a previous study, MDC treatment inhibited cell death (Schütze et al., 1999). The same group demonstrated in later work that caspase-8 is recruited to and is active at endosomal vesicles (Schneider-Brachert et al., 2004), supporting our finding that the activation of caspase-8 is downstream of endocytosis. It was not possible to reveal whether activation of caspase-8 occurs at the cytosolic face of a vesicular membrane (Tchikov et al., 2011) or within the vesicle by the colocalization experiments. The addition of lysosomal protease inhibitors or anti-cathepsin-D reduced caspase-8 activation and nuclear fragmentation, indicating that both cysteine and aspartic cathepsins work upstream of caspase-8 activation in UVA-irradiated keratinocytes. In melanocytes, UVA-induced apoptosis is mediated by lysosomal membrane permeabilization and release of cathepsins to the cytosol (Bivik et al., 2007). It has been suggested that cathepsin D activates caspase-8 in *in vitro* experiments (Conus et al., 2008; Conus et al., 2012), which further supports our findings. Cathepsin inhibitors would not only prevent the proteolytic activity of the proteases in the lysosomes but also when cathepsins have been released to the cytosol following lysosomal membrane permeabilization. Therefore, it is possible that both lysosomal and cytosolic cathepsins participate in the activation of caspase-8. Taken together, our results indicate that the initial pro-apoptotic signaling events after UVA irradiation are dependent on exocytosis and extracellular release of aSMase. Caspase-8 activation occurs following endocytosis and is cathepsin dependent.

This is the first report showing that lysosomal exocytosis is involved in the cellular response to UVA irradiation. Previously, it has been demonstrated that lysosomes repair plasma membrane damage induced by mechanical stress and pore-forming toxins (Idone et al., 2008; Reddy et al., 2001). We found lysosomal exocytosis to result in the release of cathepsin D into the extracellular space, which has also been reported to occur in keratinocytes exposed

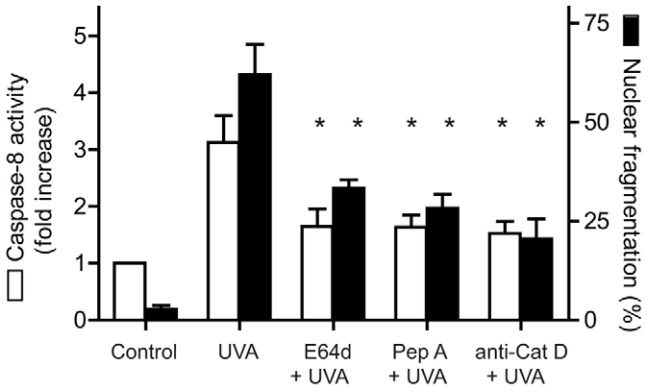

Fig. 5. Caspase-8 activation is dependent on cathepsin activity. Human keratinocytes were exposed to UVA irradiation (60 J/cm^2). Caspase-8 activity (2 hours; white bars) and nuclear fragmentation (6 hours; black bars) were analyzed after UVA irradiation. When indicated, cultures were pretreated with inhibitors of cysteine cathepsins (E64d; 10 μM, 16 hours), cathepsin D (pepstatin A; 100 μM, 16 hours) and with anti-cathepsin D antibody (anti-cat D; 42 μg/ml). *$P \leq 0.05$ compared to UVA ($n=4$).

to ionophores (Jans et al., 2004). Interestingly, pro-cathepsin D has been shown to have a mitogenic effect on fibroblasts when released extracellularly (Derocq et al., 2012). Cathepsins also promote tumorigenesis by stimulating tumor growth, enhancing angiogenesis and facilitating invasion (Gocheva et al., 2006). In glioma cells, the inhibition of lysosomal exocytosis prevents migration and invasion (Liu et al., 2012). Thus, it is possible that, following lysosomal exocytosis, the cathepsins outside of keratinocytes participate in UVA-induced skin damage and contribute to skin cancer progression.

We conclude that UVA, but not UVB, induces plasma membrane damage, which is repaired by lysosomal exocytosis in keratinocytes *in vitro*. Two hours after lysosomal exocytosis, we find cathepsin-dependent activation of caspase-8 and cell death that is prevented by endocytosis inhibition. These findings shed new light on the mechanisms of UVA-induced cell damage.

Materials and Methods

Cell culture and treatments

All experiments were performed according to the ethical principles of the Helsinki declaration and approved by the Ethical Committee at Linköping University, Sweden. Primary keratinocytes were obtained from foreskin circumcisions of fair-skinned donors (0–2 years of age), and pure cultures of keratinocytes were established and cultured as previously described (Andersson et al., 2001; Larsson et al., 2005).

The day prior to experiments, the cells were trypsinized and seeded at a density of 25×10^3 cells/cm^2. The cells were not cultured beyond passage 7. Where indicated, the following supplements were added: pepstatin A (100 μM, 16 hours, Sigma-Aldrich), E64d (10 μM, 16 hours; Sigma-Aldrich), NH_4Cl (10 mM, 30 minutes), MDC (200 μM, 30 minutes; Sigma-Aldrich), PAO (3 μM, 30 minutes, Sigma-Aldrich), α-tocopherol (10 μM, 48 hours; Sigma-Aldrich) anti-aSMase (120 ng/ml, Cell Signaling Technology, Beverly, MA, USA), anti-cathepsin D (42 μg/ml, Athens Research and Technology Inc., Athens, GA, USA), anti-Synaptotagmin VII (anti-Syt VII, 10 μg/ml, Synaptic Systems, Goettingen, Germany), vacuolin-1 (1 μM, 1 hour, Sigma-Aldrich), the caspase-8 inhibitor z-IETD-fmk (40 μM, 2 hours, BD Pharmingen, Franklin Lakes, NJ, USA) and the caspase-10 inhibitor z-AEVD-fmk (4 μM, 2 hours; Biovision, Milpitas, Ca, USA). Inhibition of endocytosis by MDC was verified by decreased uptake of FITC-conjugated dextran (40 kDa; 0.35 mg/ml, 4 hours; Sigma-Aldrich). Corresponding solvent controls or isotype controls for antibodies supplements were analyzed in parallel, and no interference was noted.

UV irradiation

The UVB source was a Philips TL20W/12 tube (Philips, Eindhoven, The Netherlands) emitting in the spectral range 280–370 nm with a main output between 305 and 320 nm; a Schott WG 305 cut-off filter (Mainz, Germany) was used. The UVA source was a Medisun 2000-L tube (Gröbel UV-Elektronik GmbH, Ettlingen, Germany; 340–400 nm). The output was 1.44 mW/cm^2 for UVB and 80 mW/cm^2 for UVA. Exposure was performed in PBS in the presence of Ca^{2+} unless otherwise stated. No increase in temperature in the medium was noted during irradiation. To achieve a 40–60% apoptotic frequency, the irradiation doses were titrated to 60 J/cm^2 UVA and 500 mJ/cm^2 UVB.

Plasma membrane repair assay

A previously established method to detect plasma membrane damage was used to assess plasma membrane repair (Idone et al., 2008). Briefly, cell cultures were irradiated in either Ca^{2+}-containing PBS (0.9 mM $CaCl_2$) or Ca^{2+}-free PBS supplemented with 10 mM EGTA. After UV irradiation, 5 μg/ml propidium iodide (Sigma-Aldrich) was added, and the cultures were incubated for 5 minutes. The cells were then fixed in 4% paraformaldehyde (20 minutes, 4℃) and mounted in ProLong Gold antifade Reagent supplemented with 4′,6-diamidino-2-phenylindole (DAPI; 1.5 μg/ml; Molecular Probes, Eugene, OR, USA). The specimens were analyzed using a fluorescence microscope (Olympus, Hamburg, Germany).

Immunocytochemistry

The lysosomal compartment was visualized by incubating the cells with 50 nM LysoTracker Red (Molecular Probes) for 1 hour at 37℃. Keratinocytes were prepared for immunocytochemistry as described previously (Appelqvist et al., 2011). The following antibodies were used: mouse anti-active caspase-8 (Millipore, Cork, Ireland), rabbit-anti-cathepsin D (Athens Research and Technology Inc.), and goat anti-LAMP-1 (Santa Cruz Bio-technology; Santa Cruz, CA, USA). This step was followed by incubation with the appropriate secondary antibodies conjugated to Alexa Fluor 488, Alexa Fluor 594 or Alexa Fluor 633 (Molecular Probes). Next, the cells were mounted in ProLong Gold antifade reagent with DAPI (Molecular Probes) and images were acquired at 20℃ using a Nikon C-1 confocal microscope (40×, 1.40 NA objective; Nikon, Tokyo, Japan) together with the EZC1 3.7 Software (Nikon) or a Zeiss LSM laser scanning confocal microscope (63×, 1.4 NA objective; Carl Zeiss AG, Oberkochen, Germany), where image analysis was performed using the Zen software (Carl Zeiss AG). Separate scans from the green and red channels were overlaid, and the colocalization coefficients (i.e. the portion of pixels from the red channel for which the intensity in the green channel contributes to the colocalized area) were collected (Bolte and Cordelières, 2006). At least 50 cells were analyzed in each sample. Negative controls, which were incubated without the primary antibody, showed no staining.

For triple staining of active caspase-8 (mouse antibody, followed by goat anti-mouse Ig conjugated to Alexa Fluor 488), LAMP-1 (goat antibody, followed by donkey anti-goat Ig conjugated to Alexa Fluor 633) and cathepsin D (rabbit antibody, followed by goat anti-rabbit Ig conjugated to Alexa Fluor 594) all secondary antibodies were added simultaneously. However, the donkey anti-goat antibodies had been pre-adsorbed against mouse and rabbit immunoglobulins in order to minimize cross-reactivity.

To detect the luminal part of LAMP-1 at the plasma membrane, staining was performed on unfixed cells. Endocytosis was blocked by adding ice-cold 5% FBS in PBS, and the samples were incubated for 5 minutes on ice. The cells were then incubated with a primary antibody (2 hours, 4℃), followed by fixation and incubation with a secondary antibody as described above. Quantifications were based on at least 100 cells in randomly selected areas.

Analysis of protein release from the cells

Immediately after UV exposure, the whole volume of the PBS medium was centrifuged at 3200 ***g*** for 10 minutes to remove cellular debris. The supernatant was concentrated using Amicon® Ultra-4 centrifugal devices (Millipore) at 4000 ***g*** (40 minutes, 4℃). To detect TNF-α, the concentrated medium was added to an anti-TNF-α ELISA (Thermo Scientific, Rockford, IL, USA) according to the manufacturer's description. For western blot analysis, sample buffer (5% β-mercapto-ethanol in Laemmli sample buffer; Bio-Rad Laboratories, Hercules, CA, USA) was added and the samples were subjected to immunoblotting as described elsewhere (Appelqvist et al., 2011; Appelqvist et al., 2012b). The following primary antibodies were used: anti-cathepsin D (Athens Research and Technology Inc.) or anti-aSMase (Cell Signaling Technology). Glyceraldehyde-3 phosphate dehydrogenase (GAPDH; Biogenesis, Pool, UK) release was monitored as a control of cellular lysis. Protein bands were visualized in the western blotting Luminol reagent (Santa Cruz Biotechnology).

Apoptosis analysis

At specified time points, the cultures were fixed and mounted in ProLong Gold mounting medium with DAPI. The nuclear morphology of 100 randomly selected cells was evaluated using a fluorescence microscope. Caspase-8 and caspase-3 activities were analyzed using the substrate Ac-IETD-AFC or Ac-DEVD-AMC, respectively, according to the manufacturer's recommendation (BD Pharmingen). The fluorescence was analyzed in a VICTOR 1420 multiple counter (Wallac Turku, Finland) and correlated to protein content.

Acid-sphingomyelinase activity assay

The Amplex® Red sphingomyelinase assay kit (Molecular Probes) was used to analyze aSMase activity in cells according to the manufacturer's instructions. Fluorescence

was analyzed in a VICTOR 1420 multiple counter (λ_{ex} 530–560, λ_{em} 590, Wallac), correlated to protein content and expressed in arbitrary units per μg protein.

Detection of lipid rafts

The cells were incubated with the fluorescent cholera toxin subunit B conjugate (Molecular Probes) for 10 minutes at 4℃, and then washed in PBS and cross-linked with the antibody against cholera toxin B for 15 minutes at 4℃. The samples where then processed for fluorescence microscopy.

Determination of lipid peroxidation

The lipid peroxidation products malondialdehyde and 4-hydroxyalkenals were measured in cells directly after UV exposure. The cells were lysed by three cycles of freeze-thawing and analyzed using the colorimetric Bioxytech LPO-586 assay (Oxis International Inc., Foster City, CA, USA). The reagents were added to the samples according to instructions from the supplier, incubated at 45℃ for 60 minutes and then centrifuged at 15,000 ***g*** for 10 minutes. The supernatant was monitored at 586 nm, and the concentration of lipid peroxidation products (malondialdehyde and 4-hydroxyalkenals) was calculated from a standard curve.

Statistics

All experiments were repeated at least three times using keratinocytes from different donors, and the results are presented as the means and standard deviations of independent samples. Statistical evaluation was performed by one-way ANOVA test, followed by Bonferroni's multiple comparison post-test for comparison between groups. Differences were considered significant when $P \leq 0.05$ and are indicated with asterisks in the figures.

Acknowledgements

We thank Anna Södergren for participating in the setup of our UV-induced lysosomal exocytosis model.

Author contributions

K.Ö., P.W. and H.A. designed the study, P.W., I.E., H.A. and K.Ö. performed the experiments and analyzed data, and H.A., K.Ö., P.W. and I.R. wrote the paper.

Funding

This study was supported by funding from the Swedish Research Council; Östergötland läns Landsting; the Welander-Finsen Foundation; and the Swedish Cancer Society [grant number 2011/636]. Deposited in PMC for immediate release.

Supplementary material available online at
http://jcs.biologists.org/lookup/suppl/doi:10.1242/jcs.130633/-/DC1

References

Akazawa, Y., Mott, J. L., Bronk, S. F., Werneburg, N. W., Kahraman, A., Guicciardi, M. E., Meng, X. W., Kohno, S., Shah, V. H., Kaufmann, S. H. et al. (2009). Death receptor 5 internalization is required for lysosomal permeabilization by TRAIL in malignant liver cell lines. *Gastroenterology* **136**, 2365-2376, e1-e7.

Andersson, E., Vahlquist, A. and Rosdahl, I. (2001). Beta-carotene uptake and bioconversion to retinol differ between human melanocytes and keratinocytes. *Nutr. Cancer* **39**, 300-306.

Appelqvist, H., Nilsson, C., Garner, B., Brown, A. J., Kågedal, K. and Öllinger, K. (2011). Attenuation of the lysosomal death pathway by lysosomal cholesterol accumulation. *Am. J. Pathol.* **178**, 629-639.

Appelqvist, H., Johansson, A. C., Linderoth, E., Johansson, U., Antonsson, B., Steinfeld, R., Kågedal, K. and Öllinger, K. (2012a). Lysosome-mediated apoptosis is associated with cathepsin D-specific processing of bid at Phe24, Trp48, and Phe183. *Ann. Clin. Lab. Sci.* **42**, 231-242.

Appelqvist, H., Sandin, L., Björnström, K., Saftig, P., Garner, B., Öllinger, K. and Kågedal, K. (2012b). Sensitivity to lysosome-dependent cell death is directly regulated by lysosomal cholesterol content. *PLoS ONE* **7**, e50262.

Armstrong, B. K. and Kricker, A. (2001). The epidemiology of UV induced skin cancer. *J. Photochem. Photobiol. B* **63**, 8-18.

Assefa, Z., Garmyn, M., Vantieghem, A., Declercq, W., Vandenabeele, P., Vandenheede, J. R. and Agostinis, P. (2003). Ultraviolet B radiation-induced apoptosis in human keratinocytes: cytosolic activation of procaspase-8 and the role of Bcl-2. *FEBS Lett.* **540**, 125-132.

Assefa, Z., Van Laethem, A., Garmyn, M. and Agostinis, P. (2005). Ultraviolet radiation-induced apoptosis in keratinocytes: on the role of cytosolic factors. *Biochim. Biophys. Acta* **1755**, 90-106.

Bivik, C. A., Larsson, P. K., Kågedal, K. M., Rosdahl, I. K. and Öllinger, K. M. (2006). UVA/B-induced apoptosis in human melanocytes involves translocation of cathepsins and Bcl-2 family members. *J. Invest. Dermatol.* **126**, 1119-1127.

Bivik, C., Rosdahl, I. and Öllinger, K. (2007). Hsp70 protects against UVB induced apoptosis by preventing release of cathepsins and cytochrome c in human melanocytes. *Carcinogenesis* **28**, 537-544.

Bolte, S. and Cordelières, F. P. (2006). A guided tour into subcellular colocalization analysis in light microscopy. *J. Microsc.* **224**, 213-232.

Conus, S., Perozzo, R., Reinheckel, T., Peters, C., Scapozza, L., Yousefi, S. and Simon, H. U. (2008). Caspase-8 is activated by cathepsin D initiating neutrophil apoptosis during the resolution of inflammation. *J. Exp. Med.* **205**, 685-698.

Conus, S., Pop, C., Snipas, S. J., Salvesen, G. S. and Simon, H. U. (2012). Cathepsin D primes caspase-8 activation by multiple intra-chain proteolysis. *J. Biol. Chem.* **287**, 21142-21151.

Corre, I., Niaudet, C. and Paris, F. (2010). Plasma membrane signaling induced by ionizing radiation. *Mutat. Res.* **704**, 61-67.

Derocq, D., Prébois, C., Beaujouin, M., Laurent-Matha, V., Pattingre, S., Smith, G. K. and Liaudet-Coopman, E. (2012). Cathepsin D is partly endocytosed by the LRP1 receptor and inhibits LRP1-regulated intramembrane proteolysis. *Oncogene* **31**, 3202-3212.

Gocheva, V., Zeng, W., Ke, D., Klimstra, D., Reinheckel, T., Peters, C., Hanahan, D. and Joyce, J. A. (2006). Distinct roles for cysteine cathepsin genes in multistage tumorigenesis. *Genes Dev.* **20**, 543-556.

Guicciardi, M. E., Deussing, J., Miyoshi, H., Bronk, S. F., Svingen, P. A., Peters, C., Kaufmann, S. H. and Gores, G. J. (2000). Cathepsin B contributes to TNF-alpha-mediated hepatocyte apoptosis by promoting mitochondrial release of cytochrome c. *J. Clin. Invest.* **106**, 1127-1137.

Idone, V., Tam, C., Goss, J. W., Toomre, D., Pypaert, M. and Andrews, N. W. (2008). Repair of injured plasma membrane by rapid Ca^{2+}-dependent endocytosis. *J. Cell Biol.* **180**, 905-914.

Jans, R., Sartor, M., Jadot, M. and Poumay, Y. (2004). Calcium entry into keratinocytes induces exocytosis of lysosomes. *Arch. Dermatol. Res.* **296**, 30-41.

Johansson, A. C., Steen, H., Öllinger, K. and Roberg, K. (2003). Cathepsin D mediates cytochrome c release and caspase activation in human fibroblast apoptosis induced by staurosporine. *Cell Death Differ.* **10**, 1253-1259.

Köck, A., Schwarz, T., Kirnbauer, R., Urbanski, A., Perry, P., Ansel, J. C. and Luger, T. A. (1990). Human keratinocytes are a source for tumor necrosis factor alpha: evidence for synthesis and release upon stimulation with endotoxin or ultraviolet light. *J. Exp. Med.* **172**, 1609-1614.

Larsson, P., Andersson, E., Johansson, U., Öllinger, K. and Rosdahl, I. (2005). Ultraviolet A and B affect human melanocytes and keratinocytes differently. A study of oxidative alterations and apoptosis. *Exp. Dermatol.* **14**, 117-123.

Lee, K. H., Feig, C., Tchikov, V., Schickel, R., Hallas, C., Schütze, S., Peter, M. E. and Chan, A. C. (2006). The role of receptor internalization in CD95 signaling. *EMBO J.* **25**, 1009-1023.

Li, X., Gulbins, E. and Zhang, Y. (2012). Oxidative stress triggers Ca-dependent lysosome trafficking and activation of acid sphingomyelinase. *Cell. Physiol. Biochem.* **30**, 815-826.

Liu, Y., Zhou, Y. and Zhu, K. (2012). Inhibition of glioma cell lysosome exocytosis inhibits glioma invasion. *PLoS ONE* **7**, e45910.

Marrot, L. and Meunier, J. R. (2008). Skin DNA photodamage and its biological consequences. *J. Am. Acad. Dermatol.* **58 Suppl.**, S139-S148.

McNeil, P. L. (2002). Repairing a torn cell surface: make way, lysosomes to the rescue. *J. Cell Sci.* **115**, 873-879.

Reddy, A., Caler, E. V. and Andrews, N. W. (2001). Plasma membrane repair is mediated by Ca(2+)-regulated exocytosis of lysosomes. *Cell* **106**, 157-169.

Rehemtulla, A., Hamilton, C. A., Chinnaiyan, A. M. and Dixit, V. M. (1997). Ultraviolet radiation-induced apoptosis is mediated by activation of CD-95 (Fas/APO-1). *J. Biol. Chem.* **272**, 25783-25786.

Roberg, K., Johansson, U. and Öllinger, K. (1999). Lysosomal release of cathepsin D precedes relocation of cytochrome c and loss of mitochondrial transmembrane potential during apoptosis induced by oxidative stress. *Free Radic. Biol. Med.* **27**, 1228-1237.

Rodríguez, A., Webster, P., Ortego, J. and Andrews, N. W. (1997). Lysosomes behave as Ca2+-regulated exocytic vesicles in fibroblasts and epithelial cells. *J. Cell Biol.* **137**, 93-104.

Schneider-Brachert, W., Tchikov, V., Neumeyer, J., Jakob, M., Winoto-Morbach, S., Held-Feindt, J., Heinrich, M., Merkel, O., Ehrenschwender, M., Adam, D. et al. (2004). Compartmentalization of TNF receptor 1 signaling: internalized TNF receptosomes as death signaling vesicles. *Immunity* **21**, 415-428.

Schütze, S., Machleidt, T., Adam, D., Schwandner, R., Wiegmann, K., Kruse, M. L., Heinrich, M., Wickel, M. and Krönke, M. (1999). Inhibition of receptor internalization by monodansylcadaverine selectively blocks p55 tumor necrosis factor receptor death domain signaling. *J. Biol. Chem.* **274**, 10203-10212.

Simons, K. and Toomre, D. (2000). Lipid rafts and signal transduction. *Nat. Rev. Mol. Cell Biol.* **1**, 31-39.

Tam, C., Idone, V., Devlin, C., Fernandes, M. C., Flannery, A., He, X., Schuchman, E., Tabas, I. and Andrews, N. W. (2010). Exocytosis of acid sphingomyelinase by wounded cells promotes endocytosis and plasma membrane repair. *J. Cell Biol.* **189**, 1027-1038.

Tchikov, V., Bertsch, U., Fritsch, J., Edelmann, B. and Schütze, S. (2011). Subcellular compartmentalization of TNF receptor-1 and CD95 signaling pathways. *Eur. J. Cell Biol.* **90**, 467-475.

Tyrrell, R. M. (1995). Ultraviolet radiation and free radical damage to skin. *Biochem. Soc. Symp.* **61**, 47-53.

Wäster, P. K. and Öllinger, K. M. (2009). Redox-dependent translocation of p53 to mitochondria or nucleus in human melanocytes after UVA- and UVB-induced apoptosis. *J. Invest. Dermatol.* **129**, 1769-1781.